JOURNAL OF MAGNETIC RESONANCE, Series A 111, 70–76 (1994)

The Sensitivity of Experiments Which Use Gradient Pulses for Coherence-Pathway Selection

GEORG KONTAXIS,*† JONATHAN STONEHOUSE,* ERNEST D. LAUE,‡ AND JAMES KEELER*§

*Department of Chemistry, University of Cambridge, Lensfield Road, Cambridge CB2 1EW, United Kingdom; and ‡Department of Biochemistry, University of Cambridge, Tennis Court Road, Cambridge CB2 1QP, United Kingdom

Received February 28, 1994; revised May 20, 1994

The use of field-gradient pulses for coherence selection in multidimensional NMR experiments may cause a reduction in sensitivity per unit time when compared to experiments which use phase cycling. In addition, care must be taken to introduce the gradients in such a way as to retain the possibility of producing spectra with pure phase (i.e., absorption-mode lineshapes). The commonly used methods of implementing gradient pulses in multidimensional experiments are evaluated and compared with respect to these issues. These predictions are confirmed for a simple molecular system. The experimentally achieved sensitivities are also compared, on a residue-by-residue basis, for the case of different nitrogen-15 proton HSQC spectra of a 166 residue protein. © 1994 Academic Press, Inc.

There has recently been great interest shown in the use of field-gradient pulses for coherence selection in multiple-pulse NMR experiments (*1, 2*). Compared to the established method of coherence-pathway selection using phase cycling, the use of field gradients offers the possibility of obtaining higher-"quality" spectra and of allowing the spectroscopist to choose the experiment time solely on the grounds of the required signal-to-noise ratio and resolution, rather than being constrained to a minimum experiment time by the need to complete a phase cycle. Both of these advantages have been demonstrated convincingly and the latter is proving to be of particular benefit in three- and four-dimensional experiments.

The use of gradient pulses in an experiment may affect the sensitivity, and, in addition, it may be necessary to take further steps to obtain pure-phase (i.e., absorption mode) spectra. In this paper we describe the influence that different approaches to the use of field-gradient pulses have on the sensitivity of pure-phase two-dimensional NMR experiments. Most of the results we derive have been given, either implicitly or explicitly, in the original publications which described particular experiments. Here, we derive these results using a single formalism and compare the sensitivity of experiments using selection by phase cycling with that of experiments using selection by gradients. These predictions are made for the case of idealized experiments and are thus concerned with the *fundamental* aspects of the sensitivity of these experiments; the influence of relaxation, exchange, or instrumental imperfections is not considered. Two sets of experimental data are then presented. The first is for a very simple molecular system and we show that the relative sensitivities of different spectra of this system are in accord with our predictions. The second set of data is taken from the spectra of a protein, and these reveal how, in practice, the results can deviate from the ideal.

We will use the HSQC experiment (*3*) as an illustrative example; various versions of the pulse sequence are shown in Fig. 1. We consider a two-spin system, I and S, whose offsets are Ω_I and Ω_S, respectively. In its basic form, this experiment produces data which are amplitude modulated with respect to t_1; this means that the signs of the modulating frequencies in t_1 are not determined, a feature which leads to inefficient use of the available digitization. There are a number of different methods for achieving F_1 frequency discrimination and thus overcoming this problem. However, it is important to ensure that the method used also retains pure-phase lineshapes; in the case of selection with gradients this requires careful attention.

In order to compare the sensitivities of the different approaches, it is essential to ensure that (i) in each case t_1 is incremented to the same maximum value, so that the spectra have the same underlying resolution in F_1, and (ii) the *same total time* is taken by each version of the experiment (*4, 5*). It turns out that frequently more than one complete data set needs to be recorded; for example, two data sets with different modulations with respect to t_1 might be needed. In such cases, the total experiment time has to be divided between the different data sets, and to account for this we include in expressions for the amplitudes of the signals a factor f, which is the fraction of the total time spent recording each data set. If two data sets are recorded, $f = \frac{1}{2}$; if one is recorded $f = 1$. Essentially this factor represents the fraction of the total signal energy which is present in each data set. Likewise, the total noise energy

† Present address: MR Institute, Allgemeines Krankenhaus, Lazarettgasse 14, A-1090 Wien, Austria.

§ To whom correspondence should be addressed.

1064-1858/94 $6.00

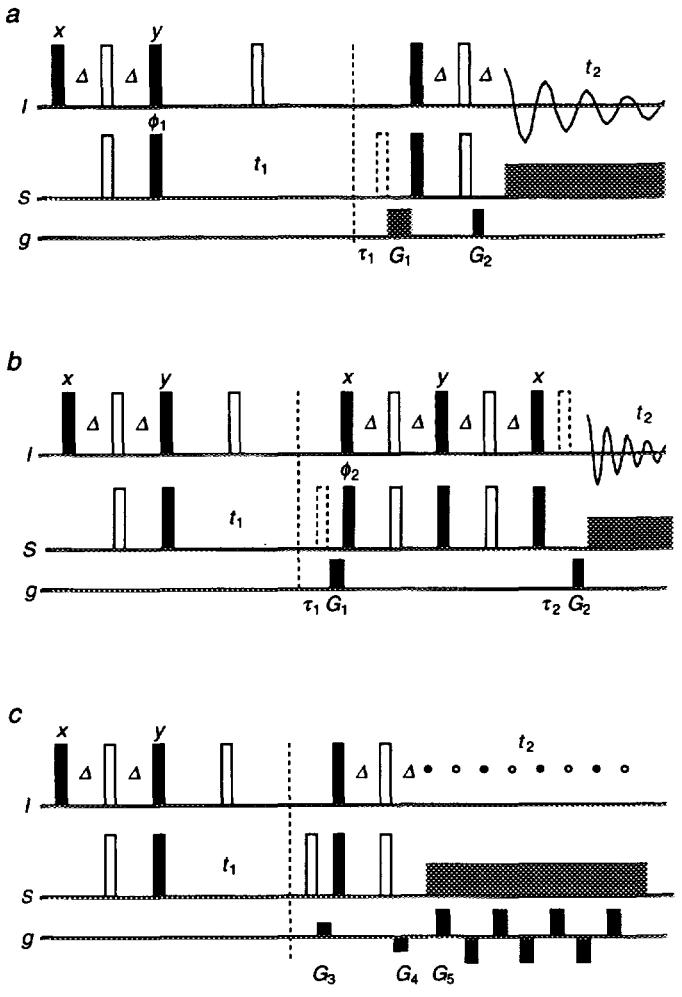

FIG. 1. Pulse sequences demonstrating how field-gradient pulses can be used in conjunction with the HSQC experiment. The 90° pulses are shown as filled rectangles, whereas the 180° pulses are shown as open rectangles; optional 180° pulses (see below) are shown as open rectangles with dashed outlines. The timing of gradient pulses is shown on the line labeled g. If the gradients, the optional 180° pulse, and the delay τ_1 are omitted, sequence (a) becomes the conventional HSQC sequence. With the inclusion of these extra items, the sequence gives rise to P- or N-type HSQC spectra, as described in the text. Sequence (b), without the gradients and optional 180° pulses, is the Cavanagh–Rance modification of the HSQC experiment; with these optional features, it is the Kay modification of the Cavanagh–Rance method. Sequence (c) is the SWAT method, in which gradients are placed between the data points that are acquired in t_2; see text for further details. Unless otherwise shown, all pulses have phase x. The delays τ_1 and τ_2 are the same as the duration of the gradients G_1 and G_2, respectively, the shaded rectangle indicates S-spin broadband decoupling during data acquisition, and the delay Δ is set to $1/(4J_{IS})$.

recorded during the experiment has to be apportioned to the different data sets; noting that the rms of the noise increases as the square root of the total experiment time, we write the rms noise level associated with each data set as $\sqrt{f}N$, where N is the rms noise level that would be observed in a single two-dimensional spectrum recorded for the entire time.

A signal which is phase modulated with respect to both times can be written

$$S(t_1, t_2) = \exp(i\Omega_1 t_1)\exp(-t_1/T_2^{(1)}) \times \exp(i\Omega_2 t_2)\exp(-t_2/T_2^{(2)}), \quad [1]$$

where $T_2^{(1)}$ and $T_2^{(2)}$ are the (assumed) exponential time constants operating during t_1 and t_2, respectively. Fourier transformation with respect to t_2 gives

$$S(t_1, \omega_2) = \exp(i\Omega_1 t_1)\exp(-t_1/T_2^{(1)})\{A_2 + iD_2\},$$

where A_2 and D_2 represent absorption- and dispersion-mode Lorentzian lineshapes, respectively, centered at Ω_2 in the ω_2 dimension. A second Fourier transformation with respect to t_1 gives the final spectrum

$$S(\omega_1, \omega_2) = \{A_1 + iD_1\}\{A_2 + iD_2\},$$

where A_1 and D_1 represent absorption- and dispersion-mode Lorentzian lineshapes, respectively, centered at Ω_1 in the ω_1 dimension. The real part of the spectrum is $A_1A_2 - D_1D_2$; this shows the *phase-twist* lineshape, which is an inextricable mixture of absorption and dispersion contributions (*6*). The intensity of the phase twist reaches its maximum on-resonance, and this intensity is entirely attributable to the double-absorption part of the lineshape, A_1A_2. For convenience we will assume that the peak height is S.

Phase modulation in t_2 is a natural consequence of quadrature detection. However, many two-dimensional experiments show amplitude modulation with respect to t_1, in the form of either cosine or sine modulation; such modulation can be written as the sum of two phase modulations:

$$\cos(\Omega_S t_1) = \frac{1}{2}[\exp(i\Omega_S t_1) + \exp(-i\Omega_S t_1)]$$

$$\sin(\Omega_S t_1) = \frac{1}{2i}[\exp(i\Omega_S t_1) - \exp(-i\Omega_S t_1)]. \quad [2]$$

FREQUENCY DISCRIMINATION IN PHASE-CYCLED EXPERIMENTS

The first method we consider is that of States, Haberkorn, and Ruben (SHR) (*7*). In this method separate cosine- and sine-modulated data sets are recorded by setting the phase ϕ_1 in the pulse sequence of Fig. 1a to x and y, respectively:

Data Set 1 (cos-modulated): $f\cos(\Omega_S t_1)\exp(i\Omega_I t_2)$

Data Set 2 (sin-modulated): $f\sin(\Omega_S t_1)\exp(i\Omega_I t_2)$. [3]

The factors f take the value one-half because half of the total experiment time is spent recording each data set; sim-

ilarly, the rms noise level associated with each data set is $N/\sqrt{2}$. For simplicity, the damping terms have been omitted and coherence order $p = -1$ is assumed to be the observable during t_2 (*8*). Fourier transformation of these two signals with respect to t_2 gives

$$\text{Data Set 1: } \tfrac{1}{2}\cos(\Omega_S t_1)[A_2(\Omega_I) + iD_2(\Omega_I)]$$

$$\text{Data Set 2: } \tfrac{1}{2}\sin(\Omega_S t_1)[A_2(\Omega_I) + iD_2(\Omega_I)].$$

A new signal is formed whose real part is the real part of Data Set 1 and whose imaginary part is the real part of Data Set 2:

$$\tfrac{1}{2}[\cos(\Omega_S t_1) + i\sin(\Omega_S t_1)]A_2(\Omega_I). \quad [4]$$

Fourier transformation of this new signal with respect to t_1 gives, in the real part, the required double-absorption-mode signal; the peak height is $S/2$. The noise level in the final spectrum remains the same as that in Data Sets 1 and 2, i.e., $N/\sqrt{2}$, since the noise levels in the real and imaginary parts of the new signal given in Eq. [4] are the same as those in the original data sets. The final signal-to-noise ratio is thus $S/(\sqrt{2}N)$.

The other commonly used method of frequency discrimination is the Marion–Wüthrich or TPPI Method (*9, 10*). In this, the coherence present during t_1 is advanced in phase by $\pi/2$ rad each time that t_1 is incremented; for the HSQC experiment this is achieved by advancing the phase ϕ_1 by 90° each time that t_1 is advanced. The increment for t_1, Δ_1, is set to half its usual value, i.e., $1/(2 \times \mathrm{SW}_1)$, where SW_1 is the spectral width in the ω_1 dimension; the resulting time-domain signal can be written

$$f\cos\left(\Omega_S + \frac{\pi}{2\Delta_1}\right)t_1\exp(i\Omega_I t_2) \quad \text{or}$$

$$f\cos\left[\Omega_S + 2\pi\left(\frac{\mathrm{SW}_1}{2}\right)\right]t_1\exp(i\Omega_I t_2). \quad [5]$$

In other words, a frequency of $\mathrm{SW}_1/2$ is added to all modulating frequencies. Thus, signals which were originally in the range $-\mathrm{SW}_1/2$ to $+\mathrm{SW}_1/2$ appear in the range 0 to SW_1. Any ambiguity over the sign of the offset is thus removed.

In the TPPI method only one data set is recorded, so $f = 1$. The data set is Fourier transformed with respect to t_2 and then the imaginary part is discarded to give the real signal

$$\left\{\cos\left(\Omega_S + \frac{\pi}{2\Delta_1}\right)t_1\right\}\{A_2\}.$$

This time-domain function is subject to a (real) cosine Fourier transform with respect to t_1, to yield a double-absorption lineshape. As the imaginary part of the data has been discarded, the peak height in the resulting spectrum is reduced by a factor of 2 to $S/2$, and the noise level to $N/\sqrt{2}$. Thus the final signal-to-noise ratio is $S/(\sqrt{2}N)$, precisely the same as that for the SHR method.

SELECTION WITH GRADIENTS

Figure 1a shows how gradients may be implemented in the HSQC sequence (*11*). Both gradients are placed within spin echoes so that any underlying evolution of the offsets (chemical shifts), which continues regardless of the dephasing and rephasing caused by the gradient pulses, is refocused. Without this refocusing, large frequency-dependent phase errors will accrue in each dimension.

An important feature of selection with gradients is that a pair of gradients can select only one coherence-transfer pathway, resulting in phase modulation with respect to the evolution in t_1. The amplitude modulation of the basic experiment, given in Eq. [3], can be considered to be the sum of two phase modulations, as shown in Eq. [2]. The phase modulation at $+\Omega_S$ arises from coherence order -1 during t_1, whereas that at $-\Omega_S$ arises from coherence order $+1$. Only one of these pathways can be refocused by the gradient pair, although we may choose which one by altering the relative sense of the two gradients. The data set in which the sense of the phase modulation is the same in t_1 and t_2 is termed the P type, and the data set in which the modulation is opposite is termed the N type. Transformation of either of these data sets gives a spectrum which is frequency-discriminated in the F_1 dimension, but which shows the undesirable phase-twist lineshape. An absorption-mode lineshape can be obtained by recording separate P- and N-type data sets:

$$\text{Data Set 1 (P-type): } \tfrac{1}{2}f\exp(+i\Omega_S t_1)\exp(i\Omega_I t_2)$$

$$\text{Data Set 2 (N-type): } \tfrac{1}{2}f\exp(-i\Omega_S t_1)\exp(i\Omega_I t_2). \quad [6]$$

As can be seen from Eq. [2], cosine modulation can be thought of as the sum of two opposite phase modulations. Gradients can be used to select just one of these modulations, hence the factors of one-half in Eq. [6]. As two data sets are recorded, $f = \frac{1}{2}$. Two-dimensional Fourier transformation of the P-type signal gives a single phase twist at (Ω_S, Ω_I), whereas the N-type signal gives a phase twist at $(-\Omega_S, \Omega_I)$. Therefore, each spectrum shows a peak height of $S/4$ and a rms noise level of $N/\sqrt{2}$.

An absorption-mode spectrum can be generated by reversing the ω_1 axis of the N-type spectrum and adding the result to the P-type spectrum (*12*). This process results in a cancellation of the dispersion parts of the phase twist, giving an absorption-mode spectrum. The signal peak height in the combined spectrum is $S/2$, and the rms of the noise again increases by a factor of $\sqrt{2}$ to N, giving a final signal-to-noise ratio of $S/(2N)$. We note that this is a factor of $\sqrt{2}$ poorer than for the SHR or TPPI methods.

A convenient strategy for processing such data is to combine the P- and N-type time-domain data to give cosine- and sine-modulated data sets which can then be processed in the usual manner used for SHR data (*13*):

Data Set 1 (cos-modulated):

(P-type data set) + (N-type data set)

Data Set 2 (sin-modulated):

$-i\{$(P-type data set) − (N-type data set)$\}$.

Subsequent data processing in the usual way for SHR data gives the same signal-to-noise ratio as that obtained by the method described in the previous paragraph.

An alternative strategy for implementing gradient selection in the HSQC experiment is to separate the first gradient from t_1 by including an extra 90° S-spin pulse at the end of t_1 (i.e., at the time indicated by the dashed vertical line in Fig. 1a). By doing this, amplitude modulation with respect to the evolution in t_1 is retained (*11*) and the SHR or TPPI method is used to achieve frequency discrimination with retention of absorption-mode lineshapes. However, it is still the case that only one pathway is refocused by the gradient pair, so that the detected signal is one-half the size that it would be for an experiment without gradient pulses (i.e., half the size of the signals given in Eq. [3]). The resulting signal-to-noise ratio is therefore one-half of that obtained in the basic phase-cycled experiment; alternatively, compared to the P- and N-type selection methods, the reduction is by a factor of $1/\sqrt{2}$. It is clear that, from the point of view of sensitivity, separating the gradient from the evolution in t_1 is not advantageous.

If gradients are used simply to destroy or purge unwanted coherences, rather than to dephase and then rephase a particular coherence-transfer pathway, there is no loss of signal intensity and signal-to-noise ratios identical to those found in the SHR or TPPI methods are to be expected (*14–17*). In the case of the HSQC experiment, a gradient can be placed between the second I-spin and the first S-spin 90° pulses. At this point in the sequence the desired magnetization is present as longitudinal spin order ($2I_zS_z$) and is thus not affected by the gradient; in contrast, the unwanted I-spin magnetization is transverse and is dephased by the gradient. Pairs of gradients can also be used in conjunction with spin echoes without any fundamental loss in sensitivity, as a refocusing pulse simply changes the sign of the coherence order and all such pathways are refocused (*2*).

SENSITIVITY-ENHANCEMENT METHODS

The SHR and TPPI methods are based on the idea that cosine- and sine-modulated data sets are available only from separate experiments. However, Cavanagh and Rance have shown that, in the case of a TOCSY experiment, it is possible to modify the sequence in such a way that *both* the sine- and the cosine-modulated signals contribute to the data recorded in a *single* experiment (*18*). Subsequently, Palmer *et al.* showed that the HSQC experiment also could be modified to give both sine- and cosine-modulated data (*19*); for convenience we will refer to this general approach as the Cavanagh–Rance (CR) modification. The modified HSQC sequence is shown in Fig. 1b. The result of the modification is that both the x and the y components of the S-spin magnetization present at the end of t_1 are transferred to the I spin and then observed. These components are sine- and cosine-modulated with respect to t_1, and, after transfer, they appear along the x and y axes at the start of t_2; as a result, the data are phase modulated with respect to t_1. Two data sets are recorded, one with the phase ϕ_2 set to $+x$ and one with the phase set to $-x$; the resulting signals can be written

$$\text{Data Set 1 } (\phi_2 = +x)\text{: } if\exp(+i\Omega_S t_1)\exp(i\Omega_I t_2)$$

$$\text{Data Set 2 } (\phi_2 = -x)\text{: } -if\exp(-i\Omega_S t_1)\exp(i\Omega_I t_2),$$

where, as two data sets are recorded, $f = \frac{1}{2}$. In effect, the two data sets correspond to P- and N-type modulations arising from the selection of coherence order −1 and +1, respectively, during t_1. Inverting the phase of ϕ_2 simply changes the sign of the signal which arises from the y component, thus making it appear as if the phase modulation is in the opposite sense.

The data are processed exactly in the same way used for P- and N-type data. Fourier transformation of each gives a spectrum containing one phase twist of height $S/2$ and an rms noise level of $N/\sqrt{2}$. The absorption-mode spectrum is recovered by reversing the ω_1 axis on one spectrum and adding it to the other. The resulting spectrum has peak of height S and a noise level of N, giving a signal-to-noise ratio of (S/N). The CR method thus gives an improvement of a factor of $\sqrt{2}$ in signal-to-noise ratio when compared to the SHR or TPPI methods. In practice, due to imperfections and the effects of relaxation, processing the data in this way is likely to give rise to quadrature images. Cavanagh and Rance (*18*) have described how these can be eliminated; the sensitivity is not affected.

Kay *et al.* have shown how it is possible to introduce gradients into experiments using the CR procedure without causing any loss in sensitivity (*20*). This possibility arises because, as has been explained above, in the CR method the two data sets already appear in the same form as the P- and N-type data sets which are generated when gradients are used. Figure 1b shows a suitable pulse sequence. Again two data sets are recorded: in the first experiment the phase ϕ_2 is set to $+x$ and the gradients are applied so as to record the N-type spectrum; in the second the phase ϕ_2 is set to $-x$ and the gradients are set to record the P-type spectrum. The resulting signals can be written

Data Set 1 ($\phi_2 = +x$, N-type): $if\exp(+i\Omega_S t_1)\exp(i\Omega_I t_2)$

Data Set 2 ($\phi_2 = -x$, P-type): $-if\exp(-i\Omega_S t_1)\exp(i\Omega_I t_2)$,

where, as two data sets are recorded, $f = \frac{1}{2}$. These are identical to those found in the CR method, so the resulting signal-to-noise ratio will be the same. It is interesting to note that the Cavanagh–Rance–Kay (CRK) method, unlike all of the other procedures for coherence selection, allows the use of gradients without any concomitant loss of sensitivity.

THE SWAT METHOD

The pulse sequence used in the SWAT method, introduced by Hurd *et al.*, is shown in Fig. 1c (*21*). In this experiment the P- and N-type pathways are refocused on alternate data points by placing gradient pulses *between the data points recorded during* t_2. Thus, in a single experiment, both P- and N-type spectra can be recorded, and these can then be processed in the manner given above to obtain an absorption-mode spectrum. During t_2 the sampling rate is set to twice its usual value so that, when the odd and even data points are separated to give the P- and N-type data sets, the sampling for each data set is at the usual rate.

The data obtained by this method are directly comparable to those obtained by recording separate P- and N-type data sets. As one data set is recorded, $f = 1$. Compared to the previous experiments, both the spectral width in the ω_2 dimension and the filter bandwidth must be doubled, and as the rms of the noise is proportional to the square root of the filter bandwidth set during acquisition, the noise level associated with each time-domain data point is increased by $\sqrt{2}$. Thus, when the time-domain data points are separated to form P- and N-type data sets, the noise level in each resulting spectrum will be $\sqrt{2}N$. Following through the argument above we find that the final signal-to-noise ratio is $S/(2N)$, identical to that obtained by recording separately the P- and N-type data. Thus, the extra complexity of SWAT seems to offer no real advantage.

EXPERIMENTAL

Experimental Verification of Calculations

Table 1 summarizes the results of a series of experiments designed to confirm our theoretical conclusions concerning the sensitivity of different experiments. The signal-to-noise ratios given in the table were measured from HSQC spectra of C_1 carbon-13-labeled glucose recorded at 600 MHz for protons; all the spectra were recorded under identical conditions and in the same total time. Broadly, these experimental results confirm our predictions, although despite careful optimization of the experimental conditions we were unable to achieve the full sensitivity improvement expected for the CR and CRK methods.

TABLE 1

Comparison of the Experimental and Theoretical Signal-to-Noise Ratios Obtained Using Different Methods of Coherence Selection and F_1 Frequency Discrimination[a]

Method	Peak height[b]	Noise level[c]	SNR[d]	Theoretical SNR
Phase cycled (SHR)	0.50	0.71	1.00	1.00
P/N selected	0.49	1.00	0.69	0.71
Cavanagh–Rance	0.96	1.01	1.35	1.41
Cavanagh–Rance–Kay	0.95	1.01	1.34	1.41

[a] Experimental data obtained from HSQC spectra of C_1 carbon-13-labeled glucose.

[b] Normalized so that the peak height found in the phase-cycled experiment is 0.5.

[c] The figure quoted is the rms of the noise, normalized to the value found in the *P/N* selected experiment.

[d] Normalized to the signal-to-noise ratio (SNR) found in the phase-cycled experiment.

In a separate series of experiments we have compared the sensitivity of conventional phase-cycled HSQC spectra with spectra recorded using the SWAT method. Using a Bruker triple-resonance probehead incorporating a single shielded-gradient coil, the maximum spectral width we could achieve without significant loss of signal intensity was 1000 Hz. The gradient pulses were of duration 320 μs and the gradient strength was estimated as 8 G cm^{-1}. Any further increase in the spectral width or the gradient strength resulted in a severe loss of signal. In agreement with the predictions made earlier, the signal-to-noise ratio of the SWAT spectrum was found to be approximately 0.7 of that of an equivalent phase-cycled experiment.

^{15}N–^1H HSQC Spectra of a Protein

The use of gradient pulses for selection inevitably results in a lengthening of the pulse sequence, and so we expect that in molecular systems where relaxation is rapid, the resulting spectra may have sensitivities which, when compared to phase-cycled counterparts, are less than predicted in the previous sections. In addition, the extra pulses which are sometimes needed in conjunction with gradients are possible sources of further loss in signal, particularly if these pulses are used for refocusing in the presence of significant off-resonance effects. In order to give some indication of what can be expected of gradient experiments in such systems, we have made a careful comparison, on a residue-by-residue basis, of the sensitivities of a series of nitrogen-15 proton HSQC spectra of the ras p-21 protein (166 residues); the results are presented in Fig. 2.

Four HSQC spectra were recorded, without presaturation of the water resonance, using pulse sequences which employ different methods of coherence selection: (i) using a single purging gradient between the second proton and first nitro-

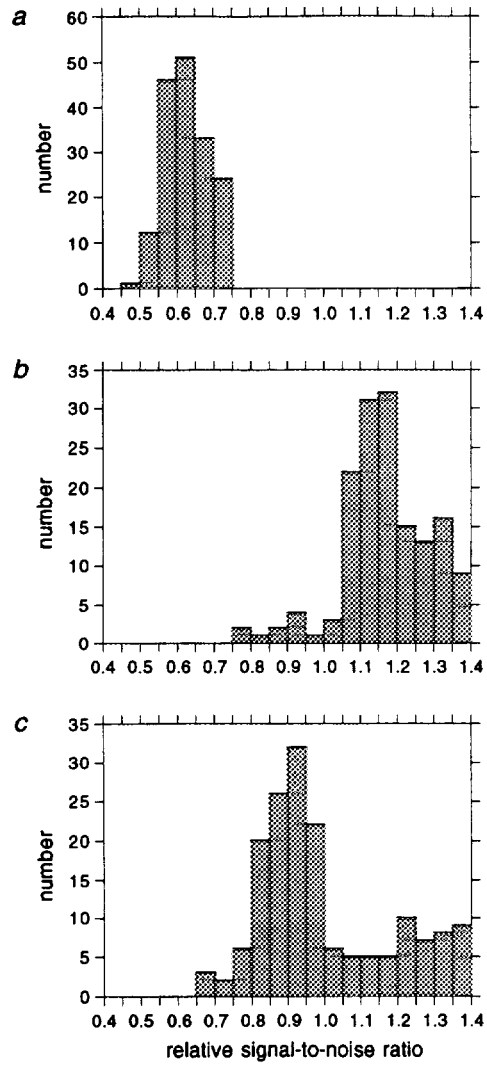

FIG. 2. Histograms illustrating the relative signal-to-noise ratios obtained from nitrogen-15 proton HSQC spectra of the ras p-21 protein (residues 1–166), complexed with GDP, recorded using different schemes for coherence selection. For each experiment and each cross peak the signal-to-noise ratio has been measured relative to that obtained from a simple HSQC spectrum (see text for details of how this was done). The height of each bar represents the number of residues with the indicated signal-to-noise ratio. Histograms (a), (b), and (c) are for the P- and N-selected, the Cavanagh–Rance, and the Cavanagh–Rance–Kay methods, respectively. The spectra from which these data were determined were recorded at 600 MHz for protons using a Bruker AMX600 spectrometer equipped with a triple-resonance probehead incorporating shielded-gradient coils. The gradient pulses had Gaussian-shaped envelopes, truncated at the 5% level, and were applied between 0.4 and 4 ms at a peak strength of approximately 10 G cm^{-1}.

gen-15 90° pulses, (ii) using a pair of gradients to generate separate P- and N-type data sets, which were subsequently processed to give an absorption-mode spectrum, (iii) using the CR method together with a single purging gradient as in (i), and (iv) using the CRK method. Each spectrum was then scaled so that the noise level, as predicted in the earlier sections, was the same; that this was so was then verified from the spectra. In these scaled spectra, the peak height is proportional to the signal-to-noise ratio. Finally, the height of each cross peak was divided by the height of the corresponding cross peak in spectrum (i). The result of this process is that we are able to determine, on a residue-by-residue basis, the signal-to-noise ratio of experiments (ii) to (iv) compared to that in experiment (i). As we have described elsewhere (*22*), the presence of significant chemical exchange between water and the NH protons can cause a loss of signal in such spectra, and so steps have been taken to ensure that any such losses are the same in each of the experiments.

Figure 2 presents our results in the form of histograms. On the horizontal axis the data bins represent different ratios of signal-to-noise between a particular experiment and experiment (i). The height of the bars indicates the number of residues whose signal-to-noise ratios fall within each binned data range. The histogram of Fig. 2a is for experiment (ii). Theoretically, the signal-to-noise ratio of this experiment should be lower, by a factor of $1/\sqrt{2}$, than that of experiment (i); as is seen from the histogram, there is a significant number of residues whose signal-to-noise ratios fall well below this figure. This effect can be attributed to the inclusion of an extra delay and a gradient during a period when the magnetization is transverse (at the end of t_1). In addition, for some residues the extra 180° pulse to nitrogen-15 may suffer from off-resonance effects.

The histogram of Fig. 2b is for the CR experiment; theoretically this experiment should have a signal-to-noise ratio which is higher, by a factor of $\sqrt{2}$, than that of experiment (i). A significant number of residues approach this ideal, and it is pleasing to note that for the vast majority of residues the CR method gives an improvement over experiment (i). The pulse sequence for the CR method is longer and contains more pulses than that for the simple HSQC; it is thus not too surprising that for some residues the enhancement is less than expected. The histogram of Fig. 2c is for the CRK method, which, like the CR method, should show a $\sqrt{2}$ improvement in signal-to-noise ratio when compared to experiment (i). It is clear that for a significant number of residues the enhancement is considerably less than the theoretical maximum. The CRK method pulse sequence is longer than that for the CR method, and it also contains two extra 180° pulses (one to proton, and one to nitrogen-15). Indeed much of the sensitivity loss of this experiment, as compared to the CR method, may be attributed to the length of the spin echo containing the first gradient pulse. In the results presented here this introduced an extra 8 ms into the sequence, during which we estimate that for the ras p-21 protein the nitrogen-15 magnetization decays typically by about 15–20%. The length of the gradient pulses should therefore be kept to a minimum so as to minimize these losses, but they must also be long enough, or strong enough, to achieve the desired level of water suppression.

These results for the ras p-21 protein can be regarded as illustrating only the differences between the experiments in a particular case. A different hardware setup or a molecular system with different relaxation times and different off-resonance effects might well give quite different results.

Although, in the present case, the CRK method failed to achieve its full promise, it should be borne in mind that this is a gradient-*selected* experiment, and thus it brings with it all the advantages that are attributed to this process. The only other gradient-selected experiment considered, in which P- and N-type data sets are recorded, gives consistently poorer sensitivity (compare the histograms of Fig. 2a and Fig. 2c). The improvement of the CRK method over nongradient-selected methods is less striking, but there are many reasons for preferring gradient selection, in which case the CRK method is advantageous.

CONCLUSIONS

It is clear from these discussions that, with the exception of experiments to which the Cavanagh–Rance–Kay method can be applied, the use of gradient pulses for coherence *selection* will result in a loss of sensitivity. This loss can be minimized to a factor of $\sqrt{2}$ by placing the gradient deliberately within the incremented time t_1; placing the gradient in any other position will cause a loss in sensitivity by a factor of two. If gradients are used for purging unwanted magnetization, or in conjunction with spin echoes, rather than for coherence selection, there is no loss in sensitivity. The SWAT method offers no sensitivity advantage when compared to placing the gradient within t_1. Finally, both the CR and the CRK methods offer a sensitivity increase of a factor of $\sqrt{2}$ over the simple (phase-cycled) SHR method. However, it should be noted that these procedures involve an increase in the length of the pulse sequence, and thus whether or not this sensitivity increase is realized fully will depend on the relaxation times of the particular molecular system under study.

ACKNOWLEDGMENTS

We thank Spectrospin (Fallenden, Switzerland) for the loan of a probe, and Dr. Joost Lohman (Bruker Spectrospin, Coventry, UK) and Dr. Detlef Moskau (Spectrospin, Fallenden, Switzerland) for their continued interest in and support of our work. We are also grateful to Dr. Sharon Campbell-Burk and Dr. Peter Domaille (DuPont Merck, Wilmington, USA) for the sample of ras p-21, and to Dr. Wayne Boucher and Robin Clowes (both of the Department of Biochemistry) for helpful discussions. G.K. thanks the Austrian Ministry for Science and Research for support, and J.S. thanks Glaxo Group Research for a scholarship. This work is a contribution from the Cambridge Centre for Molecular Recognition, which is funded by the SERC.

REFERENCES

1. R. E. Hurd, *J. Magn. Reson.* **87,** 422 (1990).
2. J. Keeler, R. T. Clowes, A. L. Davis, and E. D. Laue, "Methods in Enzymology" (N. J. Oppenheimer and T. L. James, Eds.), Vol. 239, Academic Press, San Diego, 1994.
3. G. Bodenhausen and D. J. Ruben, *Chem. Phys. Lett.* **69,** 185 (1980).
4. W. P. Aue, P. Bachmann, A. Wokaun, and R. R. Ernst, *J. Magn. Reson.* **29,** 523 (1978).
5. M. H. Levitt, G. Bodenhausen, and R. R. Ernst, *J. Magn. Reson.* **58,** 462 (1984).
6. R. R. Ernst, G. Bodenhausen, and A. Wokaun, "Principles of Nuclear Magnetic Resonance in One and Two Dimensions," Oxford Univ. Press, Oxford, 1987.
7. D. J. States, R. A. Haberkorn, and D. J. Ruben, *J. Magn. Reson.* **48,** 286 (1982).
8. G. Bodenhausen, H. Kogler, and R. R. Ernst, *J. Magn. Reson.* **58,** 370 (1984).
9. D. Marion and K. Wüthrich, *Biochem. Biophys. Res. Commun.* **113,** 967 (1983).
10. G. Drobny, A. Pines, S. Sinton, D. Weitekamp, and D. Wemmer, *Symp. Faraday Soc.* **13,** 49 (1979).
11. A. L. Davis, J. Keeler, E. D. Laue, and D. Moskau, *J. Magn. Reson.* **98,** 207 (1992).
12. P. Bachmann, W. P. Aue, L. Müller, and R. R. Ernst, *J. Magn. Reson.* **28,** 29 (1977).
13. J. Ruiz-Cabello, G. W. Vuister, C. T. W. Moonen, P. Van Gelderen, J. S. Cohen, and P. C. M. van Zijl, *J. Magn. Reson.* **100,** 282 (1992).
14. A. Bax and S. S. Pochapsky, *J. Magn. Reson.* **99,** 638 (1992).
15. B. K. John, D. Plant, and R. E. Hurd, *J. Magn. Reson. B* **101,** 113 (1993).
16. L. E. Kay, G-Y. Xu, A. U. Singer, D. R. Muhandiram, and J. D. Forman-Kay, *J. Magn. Reson. B* **101,** 333 (1993).
17. G. W. Vuister, G. M. Clore, A. M. Gronenborn, R. Powers, D. S. Garrett, R. Tschudin, and A. Bax, *J. Magn. Reson. B* **101,** 210 (1993).
18. J. Cavanagh and M. Rance, *J. Magn. Reson.* **88,** 72 (1990).
19. A. G. Palmer III, J. Cavanagh, P. E. Wright, and M. Rance, *J. Magn. Reson.* **93,** 151 (1991).
20. L. E. Kay, P. Keifer, and T. Saarinen, *J. Am. Chem. Soc.* **114,** 10663 (1992).
21. R. E. Hurd, B. K. John, and H. D. Plant, *J. Magn. Reson.* **93,** 666 (1991).
22. J. Stonehouse, G. L. Shaw, J. Keeler, and E. D. Laue, *J. Magn. Reson. A* **107,** 178 (1994).